Functional Analyses of the Plant Photosystem I-Light-Harvesting Complex II Supercomplex Reveal That Light-Harvesting Complex II Loosely Bound to Photosystem II Is a Very Efficient Antenna for Photosystem I in State II

Galka, Pierre; Santabarbara, Stefano; Thi Thu Huong Khuong, [No Value]; Degand, Herve; Morsomme, Pierre; Jennings, Robert C.; Boekema, Egbert J.; Caffarri, Stefano

Published in:
Plant Cell

DOI:
10.1105/tpc.112.100339

Publication date:
2012

Supplemental Figure 1. Analysis of the PSI oligomeric state by thylakoid solubilization and fractionation on native PAGE and sucrose gradient.

A) Native PAGE analysis (color scanned) of *Arabidopsis* State I and State II thylakoids and grana membranes. Separation was performed according to (Jarvi et al., 2011), using the CN-PAGE protocol, a large pore gel and a cathode buffer containing 0.05% sodium deoxycholate/0.02% α-DM. Membranes were solubilized with either 1% digitonin (Jarvi et al., 2011) or 0.5% digitonin/0.1% αDM (as in the rest of our work) and supplemented with 0.2% sodium deoxycholate before gel loading.

Identification of PSII antennae (LHCII and monomeric Lhcb) and supercomplexes was done by separation on a second dimension (*panel C* and *D*) and by comparison to previous results (Caffarri et al., 2009); a similar nomenclature as in (Caffarri et al., 2009) is used.

By comparing State I and State II lanes, we found in our gel only one differential band, which corresponds to the PSI-LHCII supercomplex. A faint band just above the PSI-LHCII complex is also visible in State II samples, but in this case a similar but less intense band is also present in State I thylakoids. See *panel C* and *D* for further information. No other differential band was detected in the gel suggesting the absence of other PSI-LHCII supercomplexes or PSI-LHCII-PSII megacomplexes.

B) the same gel as in *panel A* detected by fluorescence imaging (excitation in the blue region by using a UV conversion screen with max at 455 nm and FHWM of 45 nm; emission in the red region by using a long pass filter > 600 nm). Lhcb antennas show high fluorescence levels due to their very long average excited state lifetime. Similarly, PSII supercomplexes appear enhanced as compared to PSI complexes, due to their longer average excited state lifetime (see for instance B6 and B8 in the "grana" lane). Conversely, PSI and PSI-LHCII complexes are damped with respect to PSII bands (this is very clear by comparing PSI to PSII complexes having a similar or even lower intensities in the color scanned figure). Putative PSI-LHCII-PSII megacomplexes should appear as faint bands when detected by fluorescence (since energy transfer from PSII to PSI is expected). We did not identify any band of this kind, supporting the absence of PSI-LHCII-PSII complexes in our gels (see also *panel C* and *D*).

C, D) Two-dimensional analyses of the solubilized thylakoids shown in *panel* A. The second dimension was performed using SDS-PAGE according to (Laemmli, 1970), but using an acrylamide/bis-acrylamide ratio of 75:1 and a total concentration of 15.5% (w/v). Urea 6 M was also incorporated. Gels were stained with Sypro Ruby.

The whole 0.5% digitonin/0.1% DM lanes were loaded in the second dimension, while only the region from PSI until the stacking gel was loaded in the case of the 1% digitonin lanes. Only few distinctive proteins useful to identify the different complexes are indicated, according to molecular weight and previous analyses (Ballottari et al., 2004; Tikkanen et al., 2006; Caffarri et al., 2009; Jarvi et al., 2011).

Note that PSI subunits are visible in many positions of the second dimension corresponding to PSI complexes located at different MW in the first dimension. Indeed, beside monomeric PSI (PSI mon.), PSI subunits are detectable as distinct bands below B8, together with B9, between B11 and B12, and, as a smearing, till the intense green band near the stacking gel. We propose that PSI in B9 position and the first band after B11 correspond to dimeric and trimeric PSI (see also *panel G*). LHCII is found together with PSI in B9 and we explain its presence as co-migration of PSI with PSII supercomplexes. Indeed PSI oligomeric complexes are expected to migrate together or near to PSII supercomplexes. As shown in *panel E*, dimeric PSI (which likely corresponds to Mc-5b in (Jarvi et al., 2011) has a MW similar to the one of the PSII C_2S_2 supercomplex. Similarly, trimeric PSI (~1700 kDa) is expected to migrate just above B11 band (PSII $C_2S_2M_2$ complex, ~1500 kDa).

The second band of PSI found near B12 could be either a PSI tetramer (based on the MW) or the PSI-NDH complex (based on previous findings (Peng et al., 2008)).

The existence of oligomeric form of PSI *in vivo* was suggested (Jarvi et al., 2011). However, if these complexes are representative of oligomeric states of PSI *in vivo* is not clear, for at least two reasons: 1) as shown in *panel* G, oligomeric forms of PSI can be obtained *in vitro* from monomeric PSI; 2) PSI dimers, trimers and tetramers were previously investigated (Boekema et al., 2001) and, due to the flipped position of PSI units, results supported the idea that such oligomeric states are not *in vivo* association but artificial ones.

We also found PSI subunits migrating below the B8 band. The more intense band, indicated as "uncharacterized PSI complex" (*), has an estimate MW of ~850 kDa, less than a dimeric PSI but more than the here investigate PSI-LHCII complex, which migrates in a clear and distinct band at about 690 kDa (see also *panel E*). Since this uncharacterized band is visible both in State I and in State II thylakoids (even if in State II seems more intense), probably it does not represent a PSI-LHCII complex with a higher number of bound LHCII as compared to the intense PSI-LHCII band investigated in this work. Moreover, investigation by electron microscopy (see Figure 8) was not able to reveal the existence of such a complex. It is possible that this band, as other ones visible between PSI and B8 (particularly clear in *panel* C), represent PSI associated with other not yet identified chloroplast proteins needed for particular functions or for its assembly. Future work will elucidate this point.

Finally, PSI is also found co-migrating with PSII in the green band found very near the stacking gel. Jarvi and co-workers (Jarvi et al., 2011) reported the presence of a very high MW green band in solubilized State II thylakoids migrating significantly below the stacking gel, which was identified as a PSI-PSII-LHCII megacomplex. We are not able to see such a band (beside the one just below our stacking gel). However by analyzing the gel shown in (Jarvi et al., 2011) and the position of other bands which can be easily identified (for instance Sc-4b likely corresponds to B10/11 in our gel), such a megacomplex must have a MW much higher than the expected MW of a simple PSI-LHCII-PSII megacomplex (~2300 kDa). Similarly, our highest green band migrates at a very high MW, thus complexes here localized are very likely big aggregates that do not represent *in vivo* megacomplexes.

We noticed also that in the B12 band of State II thylakoids there are a significant higher content of LHCII, but without enrichment of PSI. We do not know the reason for such a difference. A possible reorganization of grana membranes in State II (Chuartzman et al., 2008) with a consequent different solubilization of thylakoids may be the raison.

In conclusion, quality of the work of Jarvi and collaborators seems very good, but the lack of a control in their experiment (State I thylakoids), the difficulty to discriminate co-migration and interaction (i.e. formation of megacomplexes) and the possibility to induce megacomplexes *in vitro* does not allow a critical and univocal conclusion about their results on the existence of PSI-LHCII-PSII complexes. In our work we have no evidence of PSI-LHCII-PSII megacomplexes.

E) Gradients of State I and State II solubilized thylakoids (the ones of Figure 1) compared to a gradient containing grana membranes fractionated in the same conditions. MW of each complex is indicated based on the protein and pigment content. Note that less PSII supercomplexes are visible in the thylakoid gradients as compared to native PAGE (panel A), likely due to the different solubilization and fractionation conditions (i.e., native PAGE uses buffers as in (Jarvi et al., 2011); gradients as indicated in the method section of this article)

F) Gradients of State I and State II solubilized thylakoids fractionated on a high concentrated sucrose gradient (from an initial solution at 0.8 M, see method section). This allows a better separation of the high MW migration region (lower part of the gradient). No additional band (beside the PSI-LHCII supercomplex) is visible in the State II sample as compared the State I sample. As in Figure 1, PSI dimers and trimers are better visible in the State I sample.

G) In vitro oligomerization of PSI monomers. Purified PSI monomers concentrated and loaded on a second gradient show the formation of dimers and trimers of PSI. This effect is enhanced in presence of high detergent (as α-DM).

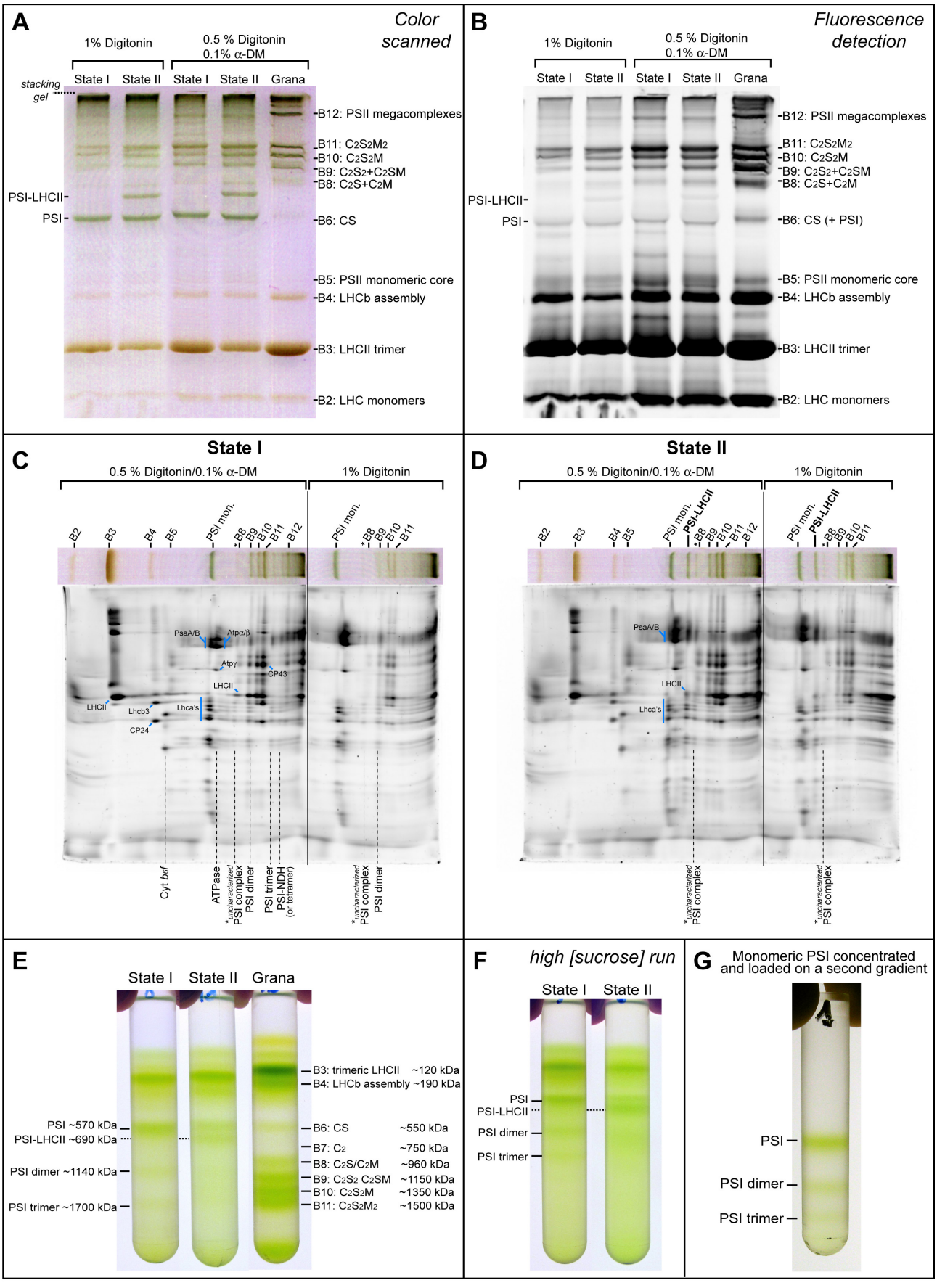

Supplemental Figure 2. Steady-state fluorescence emission spectra at room temperature for PSI and PSI-LHCII preparations.

In the PSI-LHCII complex, the LHCII excitation is efficiently trapped by PSI, but since this supercomplex is enriched in "higher energy" Chls (the ones of LHCII), it shows a stronger emission at 680 nm (LHCII) as compared to PSI. This is not visible at 77K because in this case the excited-state average lifetime of PSI increases (charge separation is slowed down and PSI fluorescence increases) and energy is rapidly concentrated and "locked" on red forms (low energy Chls), which are the main emitters at low temperature. Spectra are normalized at the maximum.

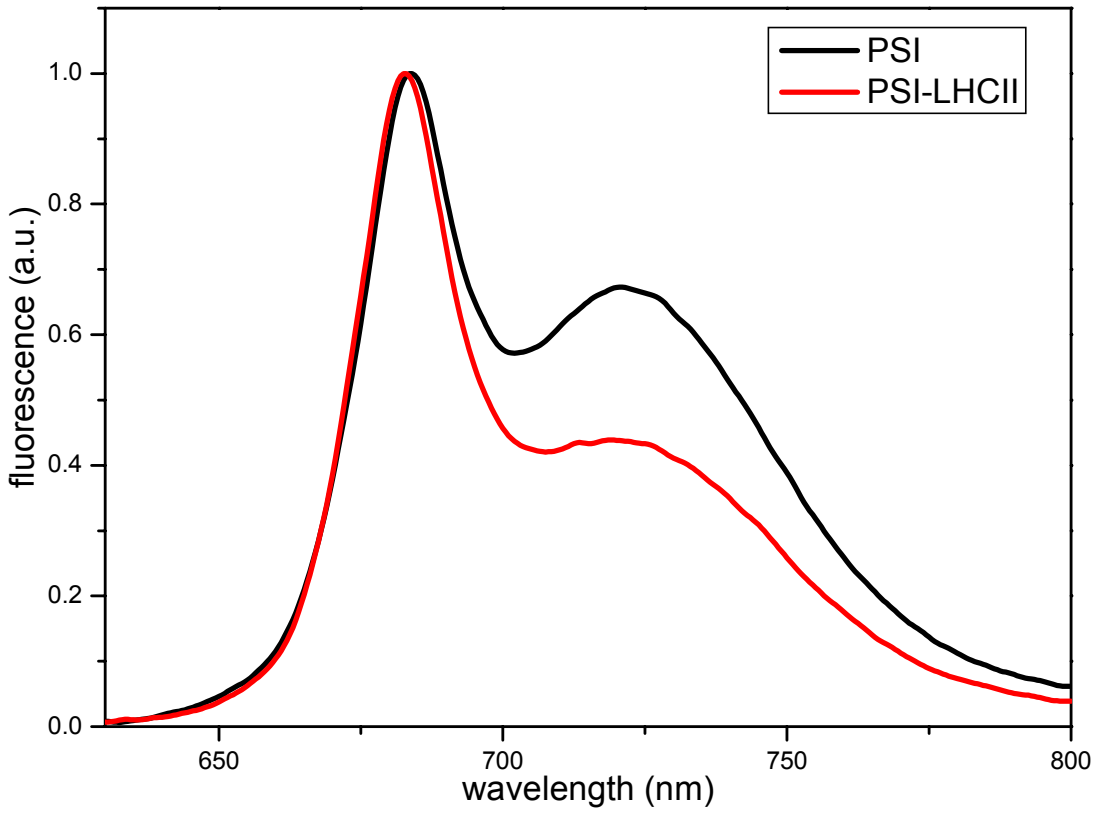

Supplemental Figure 3. Analysis of the stability of the PSI-LHCII complex. PSI-LHCII fluorescence was monitored at the maximum of the LHCII emission wavelength (680 nm) during different treatments as indicated in each panel. When the binding between LHCII and PSI is disrupted, the fluorescence yield of LHCII increases (see text). PSI-LHCII is stable at 30°C (panel A) as well as in the presence of 0.5 M NaCl (panel B). Treatment with 1 M NaCl (panel B) or 0.5% digitonin (panel C) causes some disassembly of the complex. Treatment with 0.02% α-DM has a dramatic effect on the binding stability of LHCII to PSI (panel A). A treatment with 0.2% α-DM at the end of other treatments assesses the residual level of intact PSI-LHCII. In the lower panels (E and F) the effect of a treatment of LHCII or PSI with α-DM is shown: an almost negligible effect on the fluorescence yield of the single complexes is visible. Panel G shows that the PSI-LHCII complex is stable also to freezing/thawing treatments: the frozen/thawed PSI-LHCII has the same 77K fluorescence emission as fresh PSI-LHCII, indicating that no LHCII has detached from PSI.

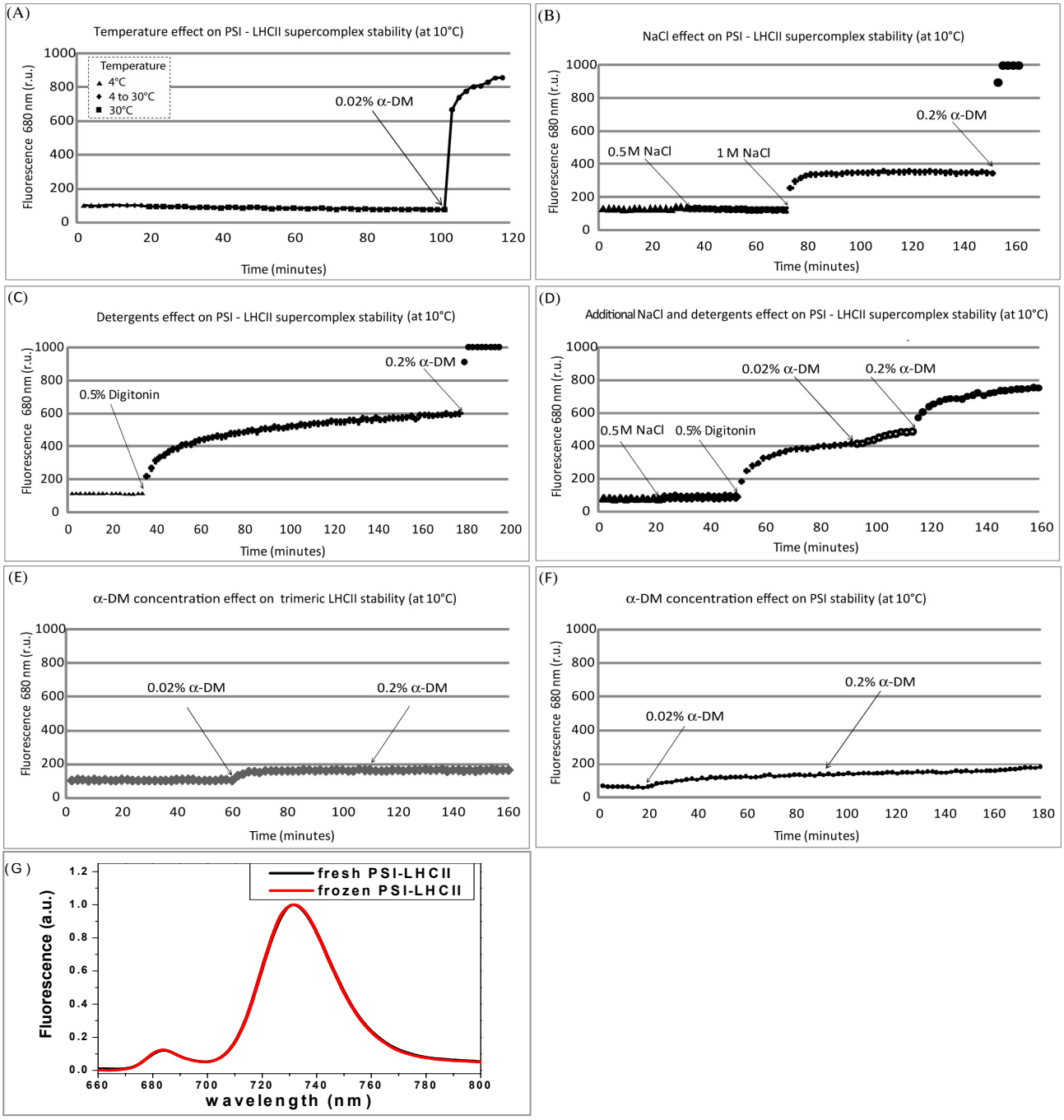

Supplemental Figure 4. Lhcb1, 2 and 3 isoform alignment and LC-MS/MS sequence coverage.

Protein sequence alignment of *Arabidopsis* Lhcb1.1-5, Lhcb2.1-4 and Lhcb3. Amino acids differing between Lhcb1.1-3, Lhcb1.4 and Lhcb1.5 are highlighted in yellow. Amino acids differing between Lhcb2.1-3 and Lhcb2.4 are highlighted in red.

Sequence coverage by MS peptides showing >96% confidence is indicated: total Lhcb1, black boxes; total Lhcb2, red boxes; Lhcb3, green boxes; Lhcb1.4, orange box; Lhcb1.4+Lhcb1.5, violet boxes.

The region in the blue box, common to all Lhcb1, 2 and 3 isoforms, has been used for normalisation of the MS areas of the same peptides from S, M and mobile trimers analysis.

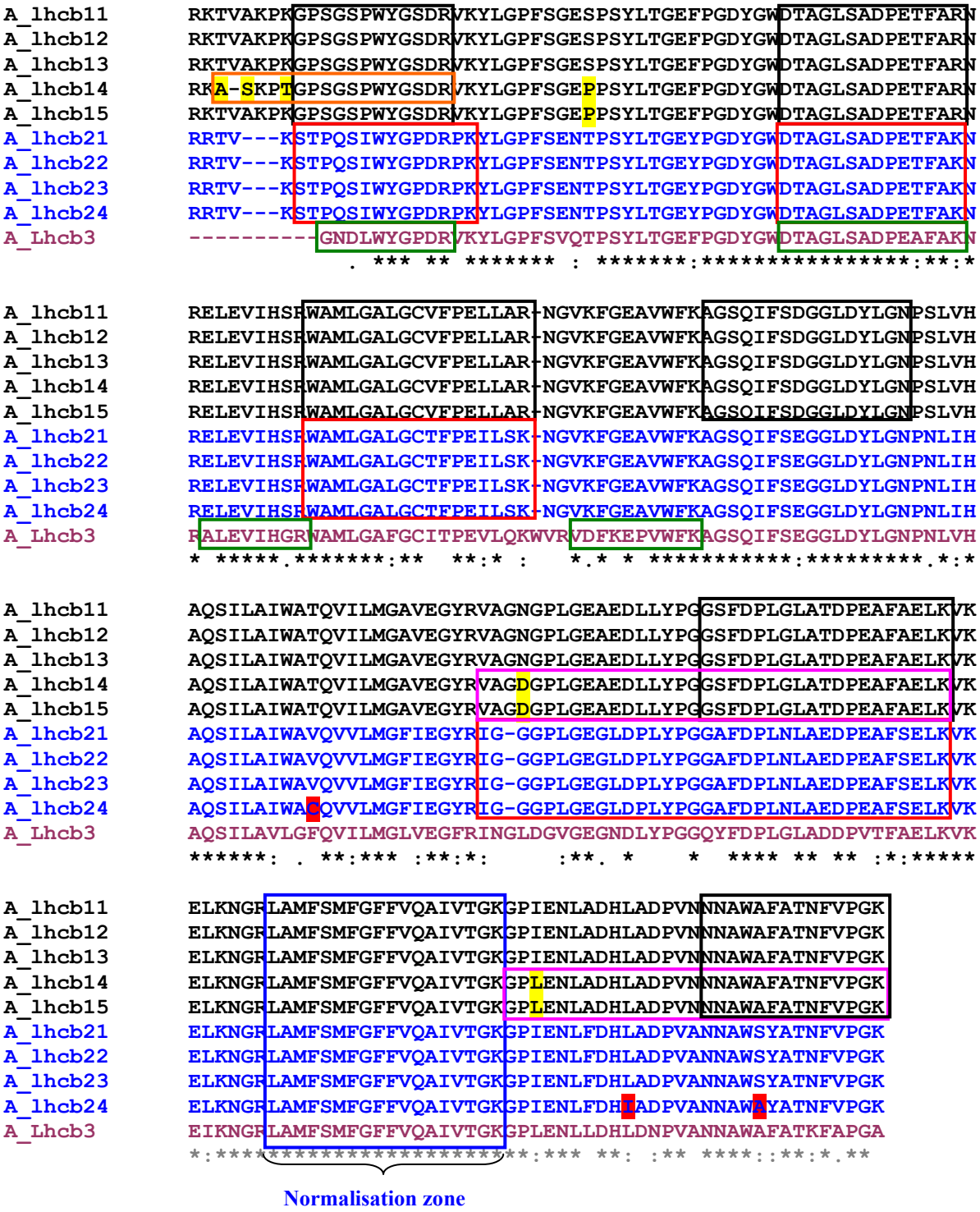

Supplemental Figure 5. Circular-dichroism spectra of PSI, PSI-LHCII and LHCII from *Arabidopsis*. Spectra were normalised to the same molar concentration (main graph). The difference spectrum "PSI-LHCII" minus ("PSI" + "LHCII") is also reported in *inset A*; the difference spectrum of PSI-LHCII before (intact complex) and after treatment with 0.02% α-DM (to disrupt LHCII to PSI binding) is also shown in *inset A*. A negative CD signal (peak at 676 nm), very likely due to the interaction between PSI and LHCII, is visible.

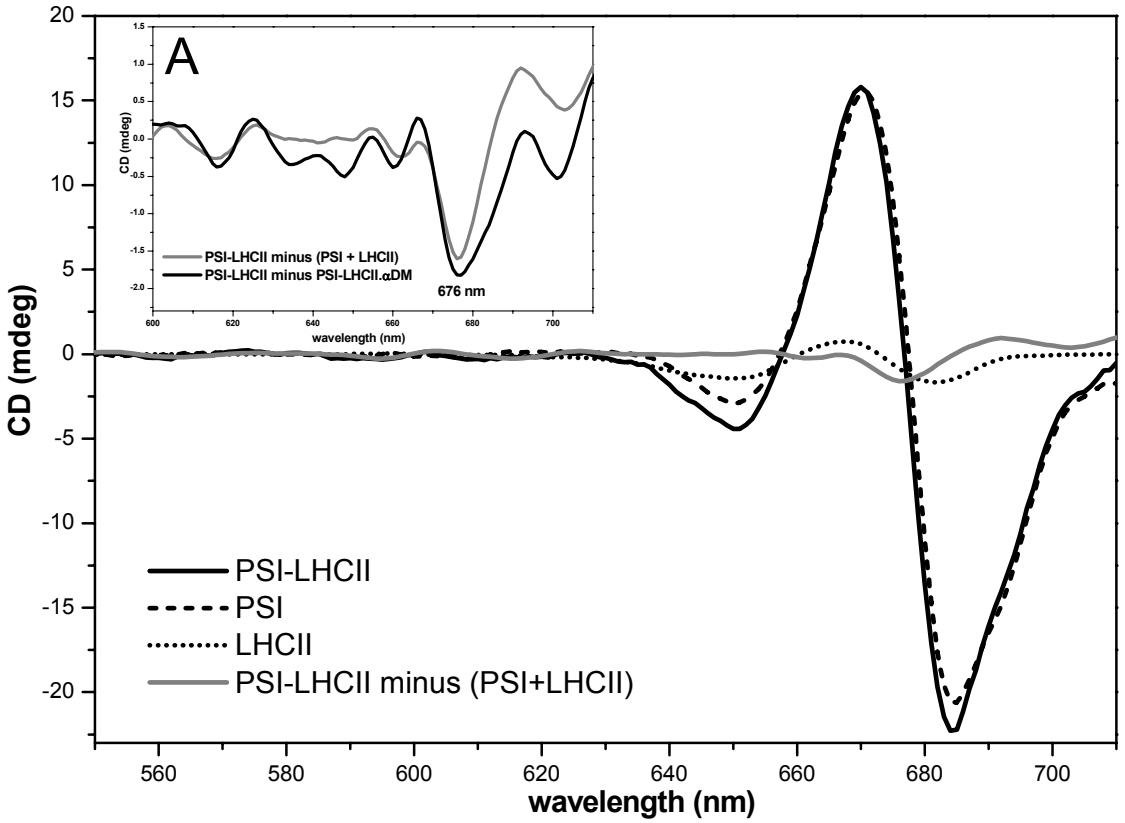

Supplemental Figure 6. Electron micrograph of purified PSI-LHCII particles. Green boxes highlight some of the pear-shaped particles representing PSI-LHCII supercomplexes. Other particles could represent differently oriented PSI-LHCII complexes, while small particles are due either to bubbles or to disassembled supercomplexes (PSI + LHCII) induced by the treatment used for the grid preparation.

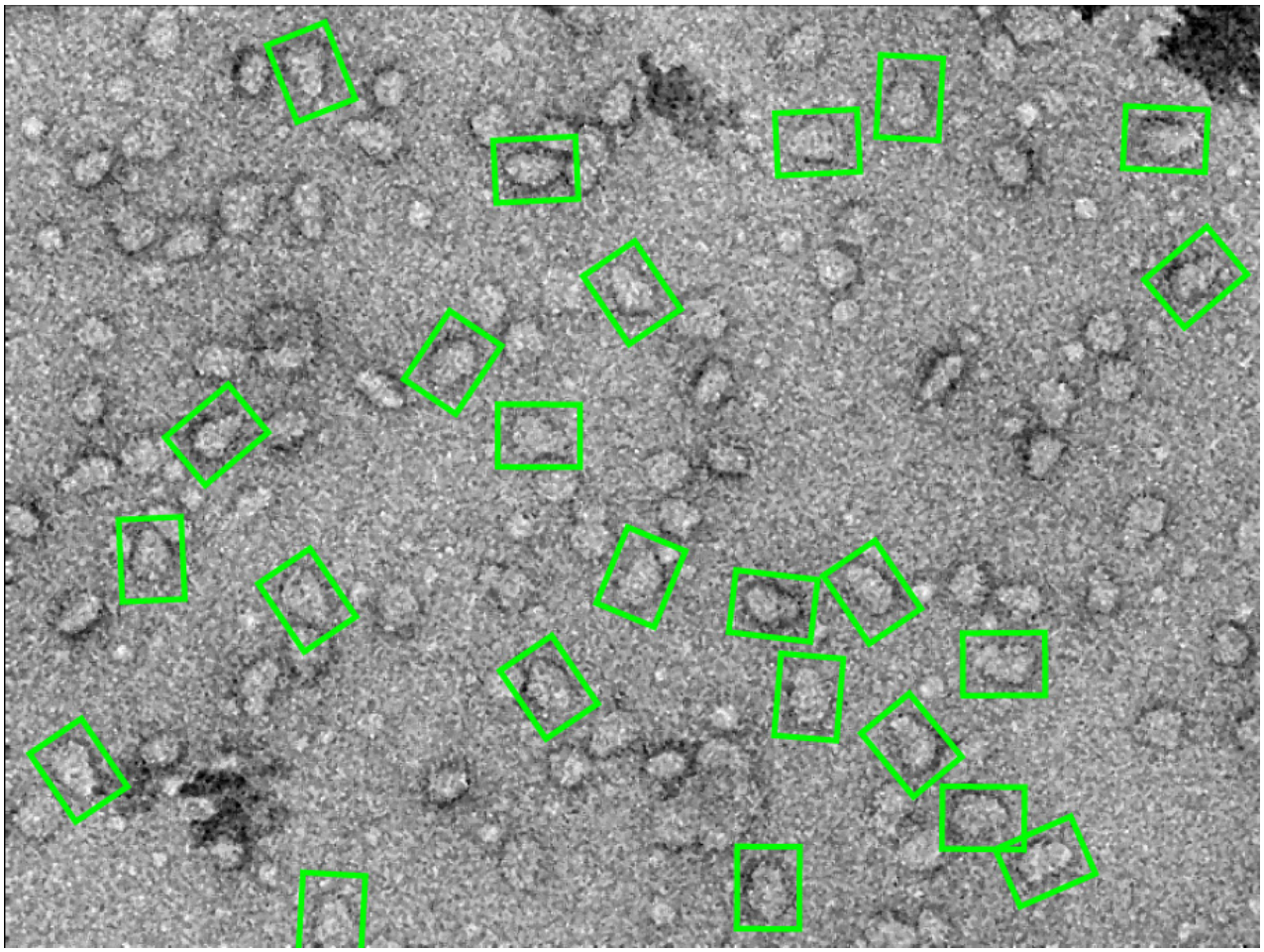

Supplemental Figure 7. Fluorescence emission spectra at 77K of thylakoids purified from *Arabidopsis* and maize plant in State I and II. Fluorescence analyses show a clear increase of the PSI emission in State II thylakoids due to the displacement of LHCII from PSII to PSI.

Fluorescence measurements were performed on thylakoids resuspended in 85% (w/v) glycerol, 10 mM Hepes pH 7.5 and cooled in liquid nitrogen, using an excitation at 475 nm. Spectra were normalized at the PSII maximum emission.

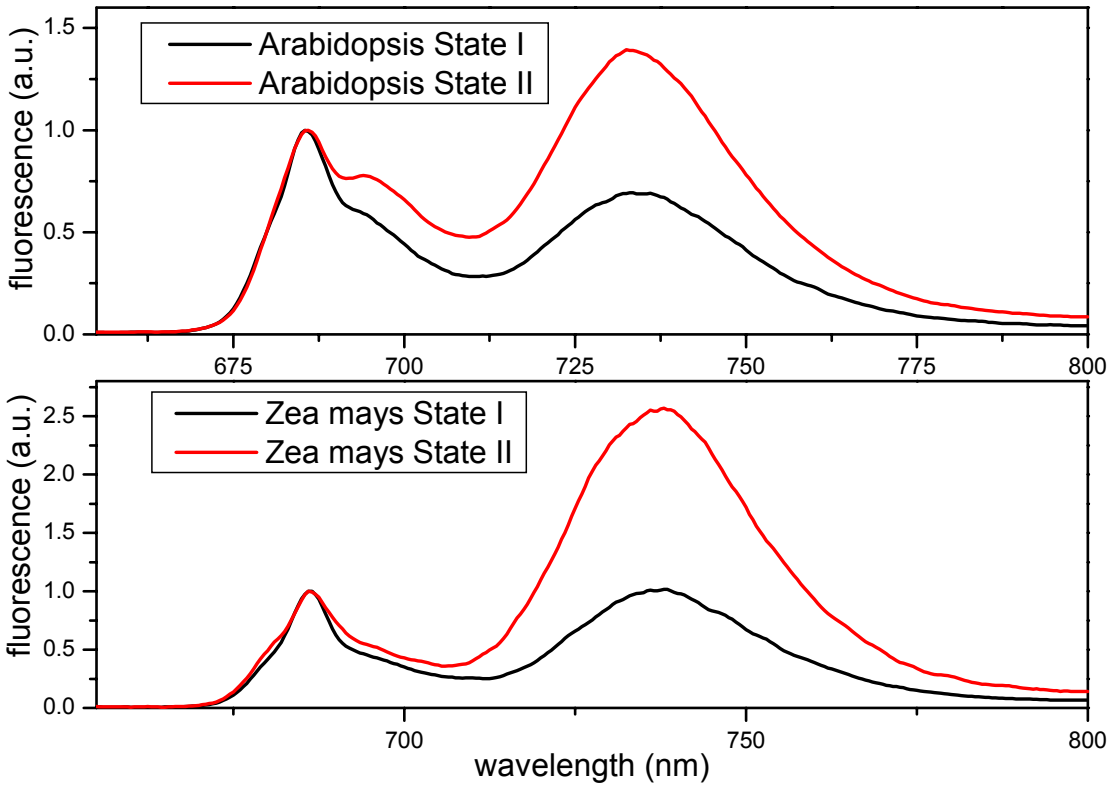

Supplemental Figure 8. Analysis of the dephosphorylation of LHCII using CIP phosphatase.

Similar amounts of PSI-LHCII complexes were loaded on a SDS-PAGE gel before (P) and after phosphatase treatment (unP, treatment with the CIP phosphatase for 2 hours). Proteins were both stained with Sypro Ruby and probed with the anti-phosphotreonine antibody (Q7, Qiagen). As clearly visible, the treatment was effective in dephosphorylating LHCII proteins.

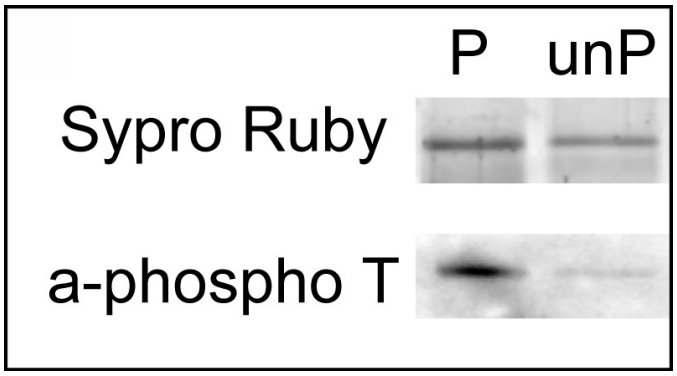

REFERENCES

Ballottari, M., Govoni, C., Caffarri, S., and Morosinotto, T. (2004). Stoichiometry of LHCI antenna polypeptides and characterization of gap and linker pigments in higher plants Photosystem I. Eur. J. Biochem **271,** 4659-4665.

Boekema, E.J., Jensen, P.E., Schlodder, E., van Breemen, J.F.L., van Roon, H., Scheller, H.V., and Dekker, J.P. (2001). Green plant photosystem I binds light-harvesting complex I on one side of the complex. Biochemistry **40,** 1029-1036.

Caffarri, S., Kouril, R., Kereiche, S., Boekema, E.J., and Croce, R. (2009). Functional architecture of higher plant photosystem II supercomplexes. Embo J. **28,** 3052-3063.

Chuartzman, S.G., Nevo, R., Shimoni, E., Charuvi, D., Kiss, V., Ohad, I., Brumfeld, V., and Reich, Z. (2008). Thylakoid membrane remodeling during state transitions in *Arabidopsis*. Plant Cell **20,** 1029-1039.

Jarvi, S., Suorsa, M., Paakkarinen, V., and Aro, E.M. (2011). Optimized native gel systems for separation of thylakoid protein complexes: novel super- and mega-complexes. Biochem. J. **439,** 207-214.

Laemmli, U.K. (1970). Cleavage of structural proteins during the assembly of the head of bacteriophage T4. Nature **227,** 680-685.

Peng, L., Shimizu, H., and Shikanai, T. (2008). The chloroplast NAD(P)H dehydrogenase complex interacts with photosystem I in *Arabidopsis*. J. Biol. Chem. **283,** 34873-34879.

Tikkanen, M., Piippo, M., Suorsa, M., Sirpio, S., Mulo, P., Vainonen, J., Vener, A.V., Allahverdiyeva, Y., and Aro, E.M. (2006). State transitions revisited-a buffering system for dynamic low light acclimation of *Arabidopsis*. Plant Mol. Biol. **62,** 779-793.